Int. J. Microgravity Sci. Appl., 36 (2) (2019) 360201
DOI: 10.15011//jasma.36.360201

IIII Original Paper IIII

Finite-Size Coherent Structures in Thermocapillary Liquid Bridges

Francesco ROMANÒ [1, 2] and Hendrik C. KUHLMANN [1]

Abstract

When small particles are suspended in a three-dimensional steady incompressible flow, Lagrangian coherent particle structures can be created by dissipative mechanisms which rely either on inertia, buoyancy or particle–boundary interactions. The dissipative effect particles experience when moving close to a wall or a free surface can lead to a particular rapid attraction of the particles to periodic, quasi-periodic or strange orbits. The particle–boundary interaction dominates the accumulation of particles in thermocapillary liquid bridges of millimetric size if the particles are small, giving rise to *finite-size coherent structures*, depending on the topological template of the underlying incompressible flow. The achievements obtained in understanding finite-size coherent structures in liquid bridges are reviewed, commenting the theoretical, experimental and numerical developments over the last two decades. Moreover, open questions and perspectives of the research on finite-size Lagrangian coherent structures are discussed.

Keyword(s): Thermocapillary liquid bridge, coherent structure, particle accumulation, dissipative structure
Received 8 February 2019, Accepted 22 April 2019, Published 30 April 2019

1. Introduction

The segregation of particles in incompressible, three-dimensional flows has been extensively studied for turbulent regimes in pipes, channels and large-scale open flows. It is important in environmental flows,[1)] city planning[2)] and man-made processes.[3)] A growing attention is recently being paid to the accumulation of particles in much smaller systems which operate in laminar flow regimes. Their characteristic length scale is of the order of a micron or a millimeter at most, with nano- or micro-particles suspended in the flow. Typical applications include the control of precipitate in crystallization processes,[4)] drug delivery,[5)] and particle sorting in micron-sized and lab-on-a-chip devices.[6)]

The dynamics of a single small particle immersed in a relatively simple unbounded flow can present a wealth of striking behaviors due to the finite-size of the particle,[7)] the particle-to-fluid density mismatch[8)] or the Coriolis force in time-periodic background flows.[9)] When confined flows are considered, an additional degree of complexity is included in the dynamics of the particulate system. A particle approaching a boundary experiences a drag and a lift force which are direct results of the interaction between the particle and the boundary (see, e.g., Brenner[10)] for a particle approaching an indeformable boundary). Thus, if the majority of particles frequently move at a distance from the boundary comparable to the particle radius, the particle–boundary interaction cannot be neglected when accurate predictions of the evolution of the particulate system are aimed at.

An example of a closed laminar flow system for which a strong particle segregation is frequently reported, is the thermocapillary liquid bridge. Suspending micron-sized particles in a millimetric liquid bridge made from a molten salt Schwabe et al.[11)] observed that the particles arranged themselves along a closed rotating periodic thread which was wrapped about the main thermocapillary vortex. The authors termed this phenomenon *particle accumulation structure* (PAS). Among the most surprising characteristics of this phenomenon was the very fast attraction, within a few seconds, of the particles to the coherent structure, despite of the small particle-to-fluid density mismatch and the very small Stokes number, $\mathrm{St} = \mathscr{O}(10^{-5})$, of the particles.

The typical setting in which particle accumulation is reported consists of a nominally axisymmetric thermocapillary liquid bridge in which a three-dimensional flow develops due to a hydrodynamic instability. For the high-Prandtl-number liquid bridges employed in experiments, the axisymmetry of the flow is broken at a critical value of the temperature difference.[12)] Above the threshold, clock- and counterclockwise propagating hydrothermal waves with azimuthal wave number m bifurcate supercritically from the basic flow.[13)] Slightly above the critical point the finite-amplitude hydrothermal wave is either azimuthally traveling or standing.[14)] Particle accumulation in liquid bridges has been experimentally reported only for traveling hydrothermal waves. Hence, mainly suspensions in traveling hydrothermal waves are reviewed, hereinafter.

Coherent particulate structures in liquid bridges have been characterized by Tanaka et al.[15)] and Schwabe et al.[16)] Their experiments have shown that the accumulation patterns are closed

1 Institute of Fluid Mechanics and Heat Transfer, TU Wien, Getreidemarkt 9, 1060 Vienna, Austria
2 Dept. Biomed. Eng., University of Michigan, 2123 Carl A. Gerstacker Building, 2200 Bonisteel Boulevard, Ann Arbor, MI 48109-2099, USA
(E-mail: frromano@umich.edu, hendrik.kuhlmann@tuwien.ac.at)

threads wrapped around the vortex core of the basic state. A general property of PAS is the close approach to the free surface of the particle thread. The shape of the closed thread of particles travels azimuthally with the same angular velocity as the hydrothermal wave. Individual particles are primarily transported by the underlying basic vortex flow, while they drift azimuthally only slowly. Tanaka et al.[15] demonstrated that different accumulation patterns can simultaneously coexist in the same flow and that the existence of PAS depends very sensitively on the flow parameters.

The significance of the work of Schwabe et al.[16] is the systematic variation of the aspect ratio of the liquid bridge, the particle size and the particle-to-fluid density ratio. Two fundamental observations were made: (a) only particles from a certain window of the particle size accumulate, and (b) the particle-to-fluid density mismatch is not required to observe particle accumulation, since density-matched particles accumulate faster than heavier particles. Based on these two fundamental results, Hofmann and Kuhlmann[17] proposed a reduced-order model to predict the accumulation of particles by modeling the particle interaction with the free surface by an inelastic collision. This model is based on the motivated assumption that a finite-size particle cannot deform nor penetrate the interface in the liquid bridges investigated. Therefore, the particle centroid must stay away from the interface by (at least) a particle radius which, in turn, was taken as the only parameter of their inelastic collision model. In their numerical flow simulations of the hydrothermal waves they found regions of regular and chaotic streamlines in the co-rotating frame of reference and explained PAS by a transfer of particles, via the inelastic particle–boundary collision, from the chaotic to a regular region of the flow. The creation of attractors by the dissipative particle–boundary interaction has recently been confirmed by the two-dimensional fully-resolved simulations of Romanò and Kuhlmann.[18] The authors employed the smoothed-profile method[19] to simulate the particle–boundary interaction based on the Navier–Stokes equations only, without invoking any interaction model. Based on their fully-resolved results,[18] they proposed a fit for determining the only scalar parameter, i.e. the minimum distance between the particle centroid and the liquid–gas interface, of the model of Hofmann and Kuhlmann[17] and validated their fit by comparison with experiments.[20]

Further advancements in the understanding of coherent structures in liquid bridges were made by Muldoon and Kuhlmann,[21] who employed a closed-form model flow to investigate the effect of the particle–boundary interaction on the accumulation of particles. The closed form of the flow allowed an extensive variation of the radius of density-matched particles, from which the authors demonstrated a wide variety of intricate scenarios depending on the particle size. A similar approach was employed by Mukin and Kuhlmann,[22] who computed the streamline topology in a three-dimensional thermocapillary liquid bridge for $\mathrm{Pr} = 4$ with much higher accuracy than Hofmann and Kuhlmann,[17] confirming the earlier results and providing more details about the accumulation process. The numerical simulations of Refs.[21,22] predicted the experimental findings of Gotoda et al.,[23] who reported the presence of a particle accumulation structure distributed along a quasi-axisymmetric attractor (known as toroidal core) and thoroughly investigated the morphing of the particle coherent structures with the Marangoni number. The numerical study of Muldoon and Kuhlmann[24] further extended the parameter space investigated, by considering a wide range of Stokes numbers St and particle-to-fluid density ratios ρ in order to compare the inertial- and the boundary-induced particle accumulation for $\mathrm{Pr} = 4$.

Other significant experimental results are due to Toyama et al.,[25] who measured the ranges of existence of particle coherent structures in a 2 cSt silicone-oil liquid bridge as function of the Marangoni number and the particle radius. Romanò and Kuhlmann[26] computed, for the first time, the flow topology of a hydrothermal wave in a high-Prandtl-number liquid bridge of $\mathrm{Pr} = 28$ and reproduced the experimental results of Toyama et al.[25] Romanò and Kuhlmann[26] correlated the particle accumulation with very slender regular regions of the flow and explained the coexistence of multiple attractors with the presence of more than one Kolmogorov–Arnol'd–Moser (KAM) torus, to which particles could be attracted. Their main achievement was the unequivocal explanation of the experimental results for the same Prandtl number by the fundamental mechanism of Hofmann and Kuhlmann.[17] They also coined the term *finite-size coherent structures* (FSCS) to emphasize PAS is a coherent structures. This notion also signals the coherent structures being due to the *finite particle size*, and not due to *particle inertia* which may lead to inertial coherent structures. A generalization of the concept of finite-size coherent structures to other boundary-driven systems was provided by Romanò et al.[27]

The remaining part of this paper is organized as follows. The problem is defined and mathematically formulated in Sec. 2. A short section, Sec. 3, is devoted to general considerations about Lagrangian-coherent structures. Experimental set-ups and numerical techniques for investigating FSCS in liquid bridges are presented briefly in Sec. 4. The main Sec. 5 presents a chronological overview of the results, subclassified to the four main research groups who have contributed to the field. Section 6 summarizes and comments the results obtained, taking stock and highlighting the necessary theoretical interpretation of the accumulation mechanism in order to be compatible with the experimental results. Section 7 reports about FSCS in other flows, and Sec. 8 proposes some applications and future perspectives of FSCS in microfluidics.

2. Statement of the problem and mathematical modeling

A liquid bridge of an incompressible Newtonian liquid is sus-

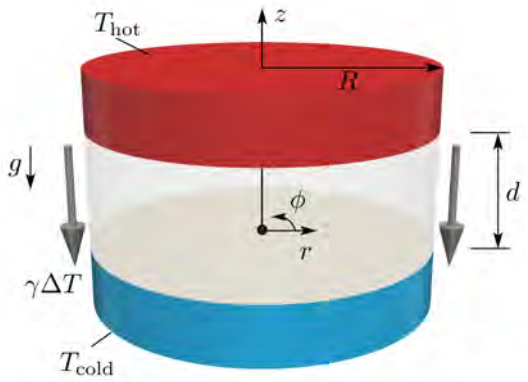

Fig. 1 Schematic of the liquid bridge, assumed cylindrical. The temperature difference ΔT between the two supporting rods induces a thermocapillary surface stress which drives the flow (gray arrows). Buoyancy forces provide an additional driving.

pended in the gap between two coaxial rods of high thermal conductivity which are separated by a distance comparable to the radius of the rods. A fluid motion is induced by tangential free-surface stresses, via the thermocapillary effect, by heating the cylinders differentially. The problem consists of predicting and measuring the flow and the motion of small spherical particles suspended in the liquid phase.

2.1 General modeling strategies

Ideally, it would be desirable to solve the Navier–Stokes equations for the moving boundary problem involving moving solids (suspended particles) and a moving liquid–gas interface between the liquid bridge and the ambient gas phase. To date the only fully-resolving numerical simulations in the above sense, including the feedback effect of the particles on the flow, have been carried out by Romanò and Kuhlmann.[18,28,29] They coupled discontinuous Galerkin-finite elements with the smoothed-profile method, as described in Romanò and Kuhlmann,[19] to compute the motion of a finite size particle in the incompressible shear flow in a cavity. Due to the large disparity of the length scales associated with the liquid bridge, the particle and the lubrication layer between particle and boundary, the simulations have been carried out for two-dimensional flows only. A fully-resolved three-dimensional simulation of a particle suspension in the liquid bridge remains prohibitively expensive, to date.

Due to this limitation, numerical simulations of FSCS usually rely on additional assumptions about the fluid- and the solid-phase. FSCS are typically observed for particles whose densities are of the same order of magnitude as that of the fluid. Moreover, the particle size is small compared to the size of the liquid bridge such that the particle-to-fluid volume fraction $\phi = \mathcal{O}(10^{-4})$ is very small. In this situation a common modeling assumption consists of neglecting the feedback of the particles on the flow as well as the mutual interaction among particles. This leads to a one-way-coupling approach,[17] where the fluid flow is solved a priori and independent of the suspended particles.

A key advantage of the one-way-coupling approach is related to the flow regime in which FSCS are found: Particle clustering in liquid bridges is only observed in traveling hydrothermal waves. If the particle moves in a hydrothermal wave without affecting this flow, the hydrothermal wave can be computed beforehand and, after being fully developed, transformed into a rotating frame of reference in which the azimuthally traveling wave becomes steady. To compute the motion of the particles in the rotating frame of reference only a single snapshot of the fully developed hydrothermal wave is required. Hence, the flow field only needs to be computed once and can be used to vary the particle size and density. However, also the particle motion equations need to be transformed into the rotating frame of reference. This approach has been introduced by Hofmann and Kuhlmann[17] and has since been used by this group. The computational cost of these simulations is very low compared to the cost associated with particle tracking in time-dependent background flows which has been employed by other groups, see e.g. Melnikov et al.[30] or Lappa.[31] Although computationally costly, the advantage of the latter approach is the possibility to assess the effect of a transient background flow on the particle motion.

2.2 Modeling of the liquid phase

2.2.1 Bulk equations

A liquid bridge consisting of an incompressible Newtonian liquid of density $\rho_{\mathrm{f}}(T)$, kinematic viscosity $\nu(T)$ and thermal diffusivity $\kappa(T)$ is clamped between two cylindrical, coaxial rods of radius R. The rods are kept at the mutual distance d and their axes are aligned parallel to the gravity vector $\mathbf{g} = -g\mathbf{e}_z$. All material properties of the liquid are assumed temperature-dependent, where T denotes the temperature field in the liquid bridge. Both the rods are kept at constant temperatures, with the bottom rod being cold at $T_{\mathrm{cold}} = T_0 - \Delta T/2$, and the top rod being hot at $T_{\mathrm{hot}} = T_0 + \Delta T/2$, where $\Delta T = T_{\mathrm{hot}} - T_{\mathrm{cold}}$ is the temperature difference between the two rods and $T_0 = (T_{\mathrm{hot}} + T_{\mathrm{cold}})/2$ the mean temperature. For a clean interface the interfacial tension $\sigma(T)$ between the liquid bridge and the surrounding gas reads, at linear order,

$$\sigma(T) = \sigma_0 - \gamma(T - T_0), \tag{1}$$

where $\sigma_0 = \sigma(T_0)$ is the surface tension at the reference temperature T_0 and $\gamma = -\partial\sigma/\partial T|_{T=T_0}$ is the negative surface-tension coefficient. Since $\gamma > 0$ for all fluids considered, the temperature difference will drive the flow along the liquid–gas interface from the hot to the cold rod. A sketch of the liquid bridge for the particular case when the shape is cylindrical is depicted in fig. 1.

Further reference quantities can be defined by $\rho_0 = \rho_{\mathrm{f}}(T_0)$, $\nu_0 = \nu(T_0)$ and $\kappa_0 = \kappa(T_0)$. Using the thermocapillary scaling

d, $d\rho_0\nu_0/\gamma\Delta T$, $\gamma\Delta T/\rho_0\nu_0$, $\gamma\Delta T/d$ and ΔT for length, time, velocity, pressure and temperature, respectively, leads to the non-dimensional Navier–Stokes, continuity and energy equations

$$\mathrm{Re}\,(\partial_t + \mathbf{u}\cdot\nabla)\,\mathbf{u} = -\nabla p + \nabla\cdot[(\nu/\nu_0)\,\nabla\mathbf{u}] + \mathrm{Bd}\;\theta\mathbf{e}_z, \quad (2a)$$

$$\nabla\cdot\mathbf{u} = 0, \quad (2b)$$

$$\mathrm{PrRe}\,(\partial_t + \mathbf{u}\cdot\nabla)\,\theta = \nabla\cdot[(\kappa/\kappa_0)\,\nabla\theta], \quad (2c)$$

where $\mathbf{x}$ is the position vector in polar coordinates (r,ϕ,z), t the time, $\mathbf{u}$ the velocity field with polar components (u,v,w), p the pressure and $\theta = (T-T_0)/\Delta T$ the reduced temperature. From the geometry, momentum and energy balance, four non-dimensional groups arise: the aspect ratio Γ, the thermocapillary Reynolds number Re, the Prandtl number Pr and the dynamic Bond number Bd

$$\Gamma = \frac{d}{R}, \quad \mathrm{Re} = \frac{\gamma\Delta T d}{\rho_0\nu_0^2}, \quad \mathrm{Pr} = \frac{\nu_0}{\kappa_0}, \quad \mathrm{Bd} = \frac{\beta\rho_0 g d^2}{\gamma}, \quad (3)$$

where β is the coefficient of thermal expansion. Alternative to the Reynolds number, the Marangoni number $\mathrm{Ma} = \mathrm{Pr}\times\mathrm{Re}$ can be used.

2.2.2 Boundary conditions

For a free-boundary problem the conditions to be satisfied on the moving boundary are frequently simplified by meaningful approximations. Here, these assumptions concern the shape of the liquid bridge and the mechanical and thermal coupling between the liquid and the gas through the free surface.

Since the surface tension σ_0 at mean temperature is very high for the liquids used in experiments, e.g. silicone oils[32] or molten salts,[16] a good approximation consists of taking the limit of vanishing capillary number $\mathrm{Ca} = \gamma\Delta T/\sigma_0 \to 0$. In this limit any flow-induced dynamic deformations of the interface are suppressed. Extensive experimental,[33] theoretical[34] and numerical[35] validations confirm the validity of this approximation. The advantage of this approximation is the shape of the liquid bridge can be obtained without solving the bulk equations, as long as the mass transfer between the liquid and gaseous phases (evaporation or condensation) is negligible over the time scale of the simulation.

Considering that the viscosity ratio between liquid and gas is very high, the shear stresses from the gas phase can safely be neglected. Determining the shape of the liquid–gas interface $\xi(z)$ reduces to computing the static surface deformation by solving the axisymmetric Young–Laplace equation

$$\Delta p(z) = \nabla\cdot\mathbf{n} + \mathrm{Bo}\,z, \quad (4)$$

where Δp denotes the hydrostatic pressure jump across the liquid–gas inteface, $\mathbf{n}$ is the outward-pointing normal unit vector, and

$$\mathrm{Bo} = \frac{\rho_0 g d^2}{\sigma_0} \quad (5)$$

the static Bond number (neglecting the density of the gas). When $\mathrm{Bo}\to 0$, also the gravitational effects on the static surface deformation can be neglected and the liquid bridge contour is described by a catenoid profile.[36] To determine the shape of the liquid bridge by solving (4) three conditions are required. With sharp edges of the solid rods supporting the liquid bridge it is reasonable to assume pinned contact lines. Furthermore, the liquid bridge must satisfy a volume constraint, leading to

$$\xi(z=\pm 1/2) = \frac{1}{\Gamma}, \quad (6a)$$

$$\int_{-1/2}^{1/2}\xi^2(z)\mathrm{d}z = \mathscr{V}, \quad (6b)$$

with the volume ratio $\mathscr{V} = V/(\pi R^2 d)$, where V is the volume of liquid suspended between the two rods.

Once the shape of the liquid–gas interface has been determined, (2) can be solved, subject to the necessary boundary conditions for $\mathbf{u}$ and θ. Under the hypothesis that the support rods are perfect thermal conductors, the fluid-flow boundary conditions at the hot and the cold rod read

$$u = v = w = 0, \quad \theta = \pm 1/2, \qquad \text{on} \quad z = \pm 1/2. \quad (7)$$

Finally, the thermocapillary effect drives the flow by a tangential stress along $r = \xi(z)$ and also the thermal coupling between liquid and gas must be considered. Several approaches have been employed in the literature,[35] depending on the required level of fidelity of corresponding experiments. Neglecting the tangential viscous stresses exerted on the interface from the gas phase, the thermocapillary tangential stress is determined by the temperature gradient on the interface

$$\mathbf{t}\cdot\mathscr{S}\cdot\mathbf{n} + \mathbf{t}\cdot\nabla\theta = 0, \qquad \text{on} \quad r = \xi(z), \quad (8)$$

where $\mathscr{S} = \nabla\mathbf{u} + (\nabla\mathbf{u})^{\mathrm{T}}$ is the stress tensor and $\mathbf{t}$ is any of the two independent tangent vectors on the interface. The surface temperature, in turn, depends on the heat transport in both the liquid and the gas phase. If, however, the gas around the liquid bridge is almost at rest, the simplest approach is to treat the interface as an adiabatic boundary, i.e. $\mathbf{n}\cdot\nabla\theta = 0$.

Due to the substantial approximations of the boundary conditions, in particular of the thermal conditions, the quantitative agreement between models and experiments might be compromised. A quite efficient improvement of the adiabatic model consists of using Newton's law of heat transfer

$$\mathbf{n}\cdot\nabla\theta = -\mathrm{Bi}\,[\theta - \theta_{\mathrm{a}}(z)], \qquad \text{on} \quad r = \xi(z), \quad (9)$$

characterized by the Biot number $\mathrm{Bi} = hd/k$, where k is the liquid heat conductivity, h the gas heat-transfer coefficient and $\theta_{\mathrm{a}}(z)$ a suitable gas phase reference temperature distribution. This approach was recently employed by Romanò and Kuhlmann,[26]

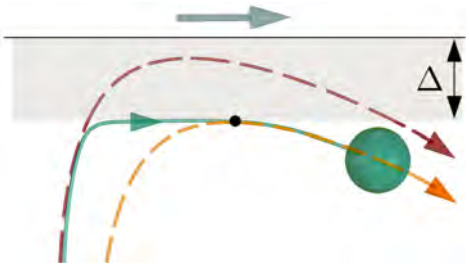

Fig. 2 Schematic of the PSI model. The particle (green sphere) which moves close to a boundary is repelled such that its centroid cannot enter a region at distance Δ from the boundary. Hence, during the collision phase, the particle trajectory (green solid line) experiences a streamline hopping from the red to the orange streamline. The black dot denotes the release point, i.e. the location where $\dot{\mathbf{y}} \cdot \mathbf{n} = 0$.

who successfully reproduced the experimental measurements of the traveling wave frequency and the FSCS in 2 cSt liquid bridges. A further improvement of the thermal boundary condition, which is slightly more costly computationally, was recently reported in Romanò and Kuhlmann,[35] who proposed an explicitly defined fit to substitute the constant Biot number in (9) by a Biot function $\mathrm{Bi}(z, \mathrm{Re}, \mathrm{Pr}, \Gamma, \ldots)$ and taking $\theta_\mathrm{a} = -1/2$, equal to the cold wall temperature. This approach is equivalent to correctly specifying $\theta_\mathrm{a}(z)$. If a higher fidelity is desired the gas-phase must be included in the simulation,[20,37] and the conditions along the liquid–gas interface turn into kinematic and dynamic boundary conditions, and an energy balance. We remark that the single-fluid approximation might be too simplistic when a coaxial gas flow is imposed on the gas phase which may lead to significant pressure gradients in the gas phase and/or cause instabilities of the liquid–gas interface.

2.3 Modeling of the solid phase

In general, the particulate phase is coupled to the fluid flow by the no-slip boundary conditions on the particle's surface. The integral of the normal and shear stresses on the particle's surface gives rise to a resultant force $\mathbf{F}$ and a torque $\mathbf{T}$ exerted on the particle. The particle trajectory can then be computed integrating the rigid-body equations which relate the translational and rotational accelerations of the particle to $\mathbf{F}$ and $\mathbf{T}$, respectively.

In the present one-way coupling, the equations of motion of the particle can be simplified under suitable conditions. Once the fluid flow is computed, the flow field $\mathbf{u}$ is employed to integrate the particle trajectory. For the motion of sufficiently small and dilute spherical particles with radius a_p the Maxey–Riley equation[38] for a single particle can be the basis for further simplifications. A widely used approximation is the simplified Maxey–Riley (SMR) equation given in Ref.[7] for the motion of the centroid $\mathbf{y}(t)$ of the particle in a given flow

$$\ddot{\mathbf{y}} = \left(\frac{1}{\rho + 1/2}\right)\left[-\frac{\rho}{\mathrm{St}}(\dot{\mathbf{y}} - \mathbf{u}) + \frac{3}{2}\frac{\mathrm{D}\mathbf{u}}{\mathrm{D}t} - \frac{\rho - 1}{\mathrm{Fr}^2}\mathbf{e}_z\right], \qquad (10)$$

where $\mathrm{D}/\mathrm{D}t$ denotes the material derivative taken in the reference frame of the flow field. In (10) the Basset history term and the Faxén corrections are neglected, as well as the Saffman lift force. When the reference frame is rotating, e.g. with the angular phase velocity of the hydrothermal wave, (10) must be transformed to the rotating frame of reference, as described in Hofmann and Kuhlmann.[17] The particle motion according to (10) depends on the non-dimensional groups

$$\mathrm{St} = \frac{2}{9}\rho \mathrm{Re} a^2, \quad \rho = \frac{\rho_\mathrm{p}}{\rho_0}, \quad \mathrm{Fr} = \frac{\gamma \Delta T}{v_0 \rho_0 \sqrt{gd}}. \qquad (11)$$

The Stokes number St is the ratio of the characteristic time of the particle to that of the fluid flow, $a = a_\mathrm{p}/d$ the dimensionless particle radius, ρ is the particle-to-fluid density ratio, and the Froude number Fr scales the buoyancy force exerted on the particle due to its density mismatch relative to the fluid.

The SMR equation (10) is a good approximation to the motion of individual spherical rigid particles if the suspension is dilute with volume fraction $\phi \leq \mathscr{O}(10^{-4})$, if the particles radius $a_\mathrm{p} \ll d$ is small compared to the domain of the flow ($\mathrm{St} \ll 1$), and if the density ratio $\rho = \mathscr{O}(1)$ is of the order of one. Furthermore, the particle Reynolds number $\mathrm{Re}_\mathrm{p} = a\mathrm{Re} \ll 1$ must be small. Since these conditions are satisfied for typical experiments, the SMR equation represents a good approximation to the particle motion as long as the particle moves far from any boundary.

Additional modeling is required when a particle moves close to a boundary, i.e., close to the support rods or the free surface. The main effect is an enhanced drag exerted on the particle in the wall-normal direction.[10] Almost all the numerical simulations which successfully reproduced experimentally observed FSCS in closed systems, employed the inelastic collision model of Hofmann and Kuhlmann,[17] the so-called particle–surface interaction (PSI) model. This phenomenological lump model becomes effective when the particle centroid is to enter a layer of thickness $\Delta \geq a$ on the boundary. Starting from this event, the normal-to-boundary velocity of the particle $\dot{\mathbf{y}} \cdot \mathbf{n}$ is annihilated as long as it is pushed towards the boundary by the flow field, i.e. as long as $\dot{\mathbf{y}} \cdot \mathbf{n} > 0$. As soon as $\dot{\mathbf{y}} \cdot \mathbf{n} \leq 0$, the PSI model switches off. This process is sketched in fig. 2. As a result, the PSI model dissipates the normal-to-boundary kinetic energy by means of an impulsive force which realizes the inelastic collision. Further considerations about this model, the interpretation of the particle–boundary interaction as a streamline hopping and the connection of the PSI model with dynamical systems theory are reported in Refs.[17,21,26]

3. Lagrangian coherent structures

Lagrangian coherent structures are distinguished trajectories or hypersurfaces in a dynamical system which have a major influence on the transport in the vicinity of these structures. In

fluid flow such a structure can be a hyperbolic point, e.g. a free stagnation point, which attracts fluid elements from some directions (stable manifold of the hyperbolic point) and deflects them in other directions (unstable manifold of the hyperbolic point). Therefore, the motion of suspended particles is largely affected by Lagrangian coherent flow structures if the particle transport is dominated by advection.

The motion of particles in a flow is governed by equations of motion which define a dynamical system. In case of an individual particle the dynamical system is given here by the SMR equation (10). In the limit of perfect advection, non-interacting particles in an incompressible flow cannot cluster, because for each particle $\nabla \cdot \dot{\mathbf{y}} = \nabla \cdot \mathbf{u} = 0$. The fluid flow and the particle flux are volume preserving. In order that particles get attracted to some attractor, dissipative effects must enter the dynamic system. In most cases such dissipative effects are due to forces which make the particles move on different trajectories than fluid elements. Typically, the forces which make dynamical system dissipative are due to the particle's inertia when $\rho \neq 1$. These forces act in the bulk of the fluid. Particulate structures which can result from inertial forces are called *inertial* coherent structures and have received much attention in recent years. Coherent structures have been subject of a focus issue of *Chaos*[39] and have been reviewed by Haller.[40]

It may happen that the dissipation leading to attractors of particles in a flow arises only in a thin boundary layer on the boundaries of the domain of the flow. The dissipative effect near boundaries can derive from the steric effect due to the finite size of the particle: The centroid of a spherical particle cannot move arbitrarily close to an indeformable boundary. Near such a boundary its normal-to-boundary motion is hindered by its finite size and additional strong normal-to-boundary drag forces arise. Since this type of dissipation is caused by the finite size of the particle, the resulting dissipative structures may be called *finite-size* coherent structure, to distinguish them form the above mentioned inertial coherent structures. Both, inertial and finite-size coherent structures are dissipative structures.

The dissipation required for particle clustering can also come form particle–particle interactions. If the dynamical system describing the whole ensemble of interacting particles exhibits attractors which become manifest in a certain particle pattern, this pattern likewise is a dissipative structure. The collective phenomenon by which interacting particles arrange themselves in a pattern can be called self-organization.

The work on particulate structures in thermocapillary liquid bridges has primarily been driven by the quest to understand the physical mechanisms responsible for the creation of the particular structures and by the desire to characterize and classify them and to detect the conditions under which such structures can exists.

4. Numerical and experimental techniques

4.1 Numerical methods

Several numerical techniques have been applied successfully to solve the equations of motion for the fluid and the particulate phase. Leypoldt et al.[13] employed a combination of finite volumes in radial and axial direction and pseudo-spectral Fourier modes in azimuthal direction in order to simulate the fluid phase neglecting the surrounding gas. The same code was used by Hofmann and Kuhlmann[17] to compute the fluid flow for $\mathrm{Pr} = 4$ and $\mathrm{Re} = 1800$. More recently, a three-dimensional finite volume solver, implemented for unstructured grids in the framework of OpenFOAM, was employed by Mukin and Kuhlmann[22] and Romanò and Kuhlmann[26]. Their calculations likewise make use of a single-fluid approach, but Ref.[26] models the thermal effect of the surrounding gas by means of Newton's cooling law, whereas Ref.[22] considered an adiabatic free surface. Romanò et al.[20] employed a finite-volume solver to compare the single- and multiphase approaches for subcritical Reynolds numbers. All these authors computed the one-way coupled particle motion a posteriori, after the flow field has become stationary. For supercritical conditions the hydrothermal wave is fully developed when it becomes stationary in the frame of reference rotating with the hydrothermal wave, provided only azimuthal harmonics of the fundamental wave number are excited. This approach has been proposed by Hofmann and Kuhlmann.[17] The particle trajectories are usually integrated by means of a Runge–Kutta method with an adaptive time step. An investigation of the numerical error arising in different time-integration schemes and its implications for particle accumulation studies can be found in Ref.[41]

Other approaches have been employed by Melnikov et al.[30] and Lappa[31]. They computed the fluid flow using finite volumes and finite differences, respectively, integrating the particle trajectories together with the fluid phase. This method requires that, at each time step, the fluid and the particle phase are integrated simultaneously in the laboratory frame of reference, without taking advantage of the fluid phase being steady in the rotating reference frame.

4.2 Apparatuses and experimental methods

The interest in thermocapillary in liquid bridges was originally stimulated by the floating-zone crystal-growth technique.[42] The liquid bridge was devised as a simplified setup to help understand the origin of striations in the crystals grown.[43] In an idealization, called *full-zone model*, the melding and solidifying interfaces are replaced by cold flat-ended cylindrical rods with an axisymmetric heater placed midway between the rods. Owing to the symmetry of the problem when gravity is disregarded, Schwabe et al.[44] introduced the *half-zone model* in which the two rods are heated differentially rather than heating from the gas phase. This setup also allowed a better control of the driving forces. Henceforth, the

half zone has become a standard system for investigating thermocapillary flow instabilities and for studying particle accumulation.

In their first experiments on particle accumulation Schwabe et al.[11] used their well-refined apparatus in which a droplet of molten $NaNO_3$ was suspended between two rods of graphite whose axes were aligned parallel to the gravity vector (heating from below). The rods of the liquid bridge had a radius of 10 mm and were coated pyrolytically. Considering that the average temperature between hot and cold rod was about 633 K, the Prandtl number of the molten salt was moderately high, i.e. $\mathrm{Pr} \approx 7$. This setup had the advantage of very little evaporation from the molten salt such that experiments could be run for hours. To investigate the particle segregation phenomenon Schwabe et al.[11] used either hollow quartz-glass spheres of radius $a_\mathrm{p} \approx 3\,\mu$m, almost density matched to the fluid (they estimated $\rho \approx 1.1$), or Al_2O_3-polishing powder ($a_\mathrm{p} \approx 7.5\,\mu$m and $\rho \approx 2.1$). In later experiments, Schwabe's group used much smaller liquid bridges in which the heater was made from sapphire to enable an axial view.[16,45] They employed $d = 2$ mm and $R = 3$ mm, a very large variety of particle shapes, and a wide range of particle diameters $a_\mathrm{p} \in [1, 60]\,\mu$m and particle-to-fluid density ratios $\rho \in [0.32, 4.8]$. Moreover, apart from molten $NaNO_3$, they also employed n-decane ($C_{10}H_{12}$, $\mathrm{Pr} \approx 15$), and 1, 2 and 5 cSt silicone oil[15] with $\mathrm{Pr} \approx 16, 28$ and 68, respectively. A typical element of Schwabe's experiments is a shield to protect the liquid bridge from external perturbations. Thermocouples embedded in the support rods were used to measure the applied temperature ΔT and very fine unshielded ones (with $30\,\mu$m wire diameter) were placed very close to the interface to extract the frequency and structure of the hydrothermal wave as well as its correlation with the particle accumulation structure.

Using a heater made from sapphire was first introduced by Kawamura et al.[46] who worked with 2 cSt silicone oil as a test fluid. Moreover, they developed a technique to carry out three-dimensional particle-tracking (3D-PTV, see Refs.[46,47]) which was also used by Tanaka et al.[15] To prevent evaporation the liquid bridge could be placed in a cold environment.[32,48,49] An alternative method to keep the volume of liquid constant is a precise control of the volume ratio (see e.g. Refs.[20,50]) which can be achieved using a micro syringe pump which refills the liquid bridge through a bore hole from the cold rod. This technique requires to measure the volume of liquid which can be achieved, for axisymmetric shapes, by image processing of suitable side-view images. Different from Schwabe's group who measured the surface temperature by fine thermocouples, Ueno's group measured the surface temperature using an infrared camera.[25] Typical test liquids employed by Ueno et al.,[32] as well as by Tanaka et al.,[15] are silicone oils produced by Shin-Etsu. Their ground experiments employed millimetric liquid bridges with $d = \mathcal{O}(1\,\mathrm{mm})$ and particles with $a_\mathrm{p} \in [2.5, 25]\,\mu$m and $\rho \in [1.7, 3.3]$.

Also Shevtsova's group carried out experiments on particle accumulation in liquid bridges, using the experimental facility inherited from Schwabe.[50] They typically employ n-decane rather than molten salts as a test liquid. In their experiments, they considered a wide range of particle radii $a_\mathrm{p} \in [0.25, 40]\,\mu$m, particle-to-fluid density ratios $\rho \in [0.95,\ 4.8]$ and several particle shapes.[51] In other setups[52–54] with very long cylindrical support rods a co-axial flow could be established in the gas phase to study its effect on the critical onset of hydrothermal waves and on particle accumulation structures.

5. Chronological overview

Particle accumulation in liquid bridges has been investigated by a number or research groups over more than two decades. Owing to the wealth of results which led to better understand finite-size coherent structures, it is worthwhile to review the achievements made regarding particle accumulation in liquid bridges. Advancements in the understanding of particle accumulation in this system have been made by only four research groups. Therefore, this review is organized in terms of these research groups, summarizing their results. Within each subsection the achievements are presented in chronological order to demonstrate how the more refined and broader view of particle accumulation has emerged from initial hypotheses and measured correlations.

At the beginning of the following literature overview, particle accumulation in liquid bridges is addressed as PAS. This is the established phenomenological nomenclature derived from the experimental observation of the particle accumulation. Towards the end of the overview, the terminology *finite-size coherent structure* (FSCS) is introduced. It emphasizes that PAS in liquid bridges is part of a more general phenomenon which is caused by the finite size of the particles. The understanding of PAS as a FSCS has evolved only recently. In section 6 the numerical, experimental and theoretical results are integrated to explain FSCS in the framework of dynamical systems and to discuss its characteristic properties.

5.1 Schwabe's group

The research interest about PAS in liquid bridges started in 1996, when Schwabe et al.[11] discovered that initially evenly distributed particles tend to accumulate and form particular persistent structures. These structures were named *particle accumulation structures* (PAS). In 1999 Schwabe[55] published a review article in which he reviewed his recent findings and elaborated on future perspectives for investigating PAS. Furthermore, Schwabe and Frank[56] characterized the behavior of particle clouds in a time-dependent thermocapillary liquid bridge, and discuss the accumulation of particles in the liquid bridge as an analogy to star formation and accretion disks. Later, when a deeper understanding of the relevant physics of PAS had evolved, this hypothetical analogy turned out to be too far-fetched.

The first experiment under microgravity conditions in which

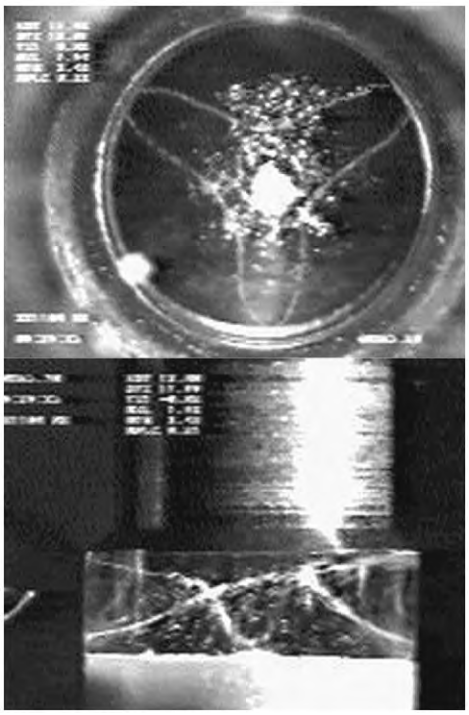

Fig. 3 Top and side view of $m = 3$ PAS with $m = 3$ under microgravity conditions.[45] The n-decane liquid bridge flow is realized for $R = 3$ mm, $d = 1.9$ mm, $\Delta T = 12$ K and the particles have $a_p = 10 - 15$ μm. The figure is taken from Schwabe et al.[16]

an unexpected particle behavior was observed was carried out in the experiment MAUS G 141 on the STS 89. Schwabe and Frank[57] reported a *sectorial PAS*[1] in steady thermocapillary flow, even though distinct particle accumulation structures of oscillatory thermocapillary convection was not observed. Together, all observations made by Schwabe's group indicated that PAS is a physical phenomenon and not some experimental artifact. In 2000, this conclusion led to the ESA-funded project AO-2000-091, "Dynamics of Suspended Particles in Periodic Vortex Flows". In the framework of this ESA project a new dedicated microgravity experiment was carried out on MAXUS-6, launched in 2006. The results, published by Schwabe et al.,[45] confirmed that PAS does not rely on buoyancy. However, gravity was found to have an effect on the parameter windows for which the particle coherent structures are observed. The main focus of the investigations of Schwabe et al.[45] was on the so-called SL1 PAS with fundamental wave number $m = 3$, which arises as a closed rotating thread of particles wrapping three times around the vortex core (fig. 3).

1 In the light of the current knowledge of FSCS this sectorial PAS may be explained by a depletion effect together with a weak azimuthal symmetry breaking.

A further confirmation of the existence of PAS under normal gravity conditions was provided by Tanaka et al.,[15] who carried out a thorough experimental study on ground for a wide range of parameters. They worked with 2 cSt silicone oil with nominal Prandtl number $\mathrm{Pr} = 28$ and reported, for the first time, the so-called SL2 PAS, another line-like particle attractor which wraps six times around the vortex core in a flow with a fundamental wave number $m = 3$. Moreover, they observed that SL1 and SL2 PAS can coexist and, reconstructing the accumulation pattern, they highlighted that PAS approaches the free surface very closely. They also reported PAS with different fundamental azimuthal wave numbers $m = 2$, 3, 4 and 5. Particles were even observed to be attracted to a toroidal core, an accumulation pattern qualitatively different from the line-like coherent structures such as SL1 and SL2 PAS. Furthermore, Tanaka et al.[15] established that the particles of the PAS do not travel azimuthally with the same velocity as the particulate pattern. Rather, particles contributing to PAS slowly drift in azimuthal direction and opposite to the azimuthal traveling direction of PAS. The direction and order of magnitude of the particle drift velocity is consistent with the azimuthal mean flow (average over the (r, φ) plane) predicted by Leypoldt et al.[13] for a traveling hydrothermal wave. Among the main achievements of Tanaka et al.,[15] the topology of PAS is almost independent of the particle-to-fluid density ratio ρ and of the Stokes number St. They also showed that the particles move almost like the fluid, indicating that the fluid flow has topological structures which are very similar to the coherent structures observed. This key feature of PAS can be understood considering that the typical Stokes numbers are very small and, therefore, a particle moves very similar as a fluid element.

Schwabe et al.[16] extended the experimental investigation of Tanaka et al.[15], reproducing PAS on the ground in liquid bridges made of mixed $NaN0_3$ and $CsN0_3$ melts, as well as bridges made of n-decane. They systematically measured (by the eye) the formation time of PAS starting from a quasi-random initial distribution of particles. The study was mainly concerned with the dependence of PAS on the particle parameters a and ρ. Two important results were experimentally established: (a) the accumulation of heavy ($\rho \geq 1$) particles is fastest when the particle is density-matched to the fluid ($\rho = 1$), and (b) only particle radii within a certain range lead to coherent particle structures, with a certain optimum particle size for which PAS forms most rapidly. The authors argued that the fast accumulation within a few periods of flow oscillation is due to inertial migration in the cross stream direction of a shear flow. Additional information was contributed by Schwabe and Mizev,[58] who reported a subcritical accumulation pattern termed toroidal shell. Confirmations as well as further investigations of this axisymmetric particle structure can be found in Melnikov et al.[59] and Romanò and Kuhlmann.[20] The most recent contribution of Schwabe is a review about thermocapillary flows[60] which includes a paragraph on PAS in liquid

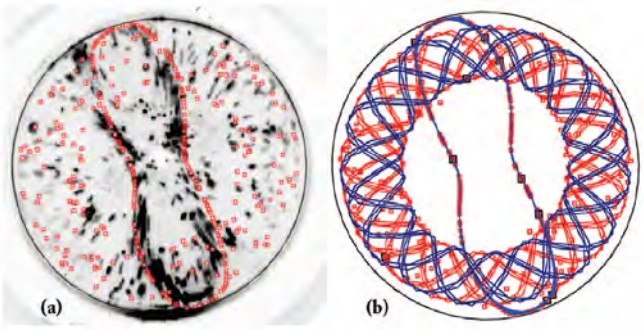

Fig. 4 Finite-size coherent structures in an n-decane liquid bridge. (a) Numerical simulation for $\Delta T = 9$ K (diamond) superposed to the experimental visualization of PAS for $\Delta T = 9.75$ K. (b) Reconstruction of ten particle trajectories in the rotating reference frame. The figure is taken from Melnikov et al.[59)]

bridges. Schwabe's group well deserves the merit of having discovered PAS and of having established its crucial dependence on a and ρ.

5.2 Shevstova's group and Lappa

The results obtained by Shevtsova's group and by Lappa are treated in a combined section, since these authors proposed very similar arguments for an interpretation of PAS. In the first investigation of the subject, Melnikov et al.[30)] carried out single-phase numerical simulations for sodium nitrate ($NaNO_3$) and n-decane liquid bridges, i.e. the fluids which have been used by Schwabe et al.[16)] Employing the SMR equation (10), the authors were able to reproduce the PAS observed in previous experiments by Schwabe's group. In order to avoid particles exit the domain, they implement the PSI model wit, setting $\Delta = a$. Based on their simulations, they concluded that the existence of line-like coherent structures is crucially related to the strength of the flow, given by the Marangoni number Ma, and to the particle-to-fluid density ratio ρ. While the dependence on Ma of PAS has been proven experimentally, the claimed importance of the density ratio is in conflict with the experimental observation of Schwabe et al.,[16)] who pointed out the existence of PAS is strongly correlated with the particle radius a, whereas $\rho > 1$ is of lesser importance for the existence of PAS as long as the particles do not settle.

In a subsequent analysis Pushkin et al.[61)] studied a model in which the flow field is given in closed form. This approach was aimed at simplifying the modeling effort, but at the same time to keep the essential physics of the experiments. This approach has some numerical advantages: The velocity field is known everywhere in the domain such that no interpolation between discrete data is required. Moreover, the background flow is available in closed form and solenoidal. Up to numerical accuracy, the latter property does not add artificial numerical dissipation to the equation of motion for the particle via the velocity field. Rather than the SMR equation (10), Pushkin et al.[61)] employed the inertial equation,[62)] which represents a simplification of (10) valid up to linear order in St. Without employing the PSI model, the authors found what they called 'self-assembly' of particles in their model flow. They concluded that this accumulation is the result of a phase-locking mechanism between fluid- and solid-phase. This conclusion has been criticized by Kuhlmann and Muldoon,[63)] who argued that a synchronization (hence phase-locking) is not possible in the one-way-coupled system of Pushkin et al.,[61)] because a necessary condition for synchronization is a *weak* mutual coupling between the particles and the fluid. Since the flow is computed independently of the particle suspension, without considering any feedback effect of the particles on the fluid flow, the mutual-weak-coupling condition is not satisfied and phase-locking cannot be responsible for the self-assembly found. Kuhlmann and Muldoon[63)] rather argue that the particles are so small $(\mathrm{St} \ll 1)$ that their trajectories must be very similar to those of fluid elements (as previously verified by the experiments of Tanaka et al.[15)]), making the particle almost slaved to the flow which is a *strong* one-sided coupling. Additional investigations of Kuhlmann and Muldoon[64)] considered a similar model flow and demonstrated that particle accumulation can be produced by inertia, by particle–boundary interaction or by both. For the experimental parameters of interest $\mathrm{St} \ll 1$ and $\rho = \mathcal{O}(1)$, they also pointed out the inertial time scale is much longer than what was experimentally measured by Schwabe et al.,[16)] whereas the clustering due to particle–boundary interaction is much faster and compatible with the experimental evidence. Kuhlmann and Muldoon[64)] employed a ninth-order integration scheme to carry out the simulations, but did not manage to reproduce the results of Pushkin et al.[61)]. In a subsequent paper, Muldoon and Kuhlmann[41)] demonstrated that particle accumulation similar to the one found by Pushkin et al.[61)] can also be caused by accumulation of numerical errors, if low-order schemes and/or large integration time steps are employed. Pushkin et al.[65)] replied to the comment of Kuhlmann and Muldoon[63)] stating that their simulations do not include any particle–boundary interaction model. Without commenting on the issue of numerically-induced coherent structures, they state the particle accumulation they observe is due to inertia and that their model cannot explain the particle coherent structures observed by Schwabe et al.[16)] for density-matched particles.

Further experimental evidence of particle accumulation in liquid bridges was reported by Melnikov et al.,[66)] who employed relatively large particles with radii $a_\mathrm{p} = 20$ and 100 μm which were 8% heavier than the liquid phase (n-decane). Even though the authors claim the clustering of particles is due to inertia and to the synchronization process between particles and fluid phase, they used one-way-coupled simulations and the PSI model of Hofmann and Kuhlmann.[17)] The use of the PSI model was seen as a necessity to keep the particle inside the computational domain, but the implications of the PSI model for the global par-

ticle motion was disregarded. Their results confirm that modeling the particulate phase by the SMR equation including inelastic boundary collision represents a good minimal model which well captures their experiments. The same approach was used in Melnikov et al.,[59] where experimental results of particle accumulation in form of a $m = 2$ PAS wrapping around a toroidal core were well reproduced by the SMR equation supplemented with the PSI model (fig. 4). They further elaborated on the phase-locking mechanism as the process responsible of the clustering of particles, even if this mechanism is in evident contradiction with the one-way coupling employed in the their numerical model.

Also Lappa[31] dwelled on the phase-locking mechanism of Pushkin et al.,[61] correlating it with the axial vorticity of the flow with the intention to validate and generalize the theoretical interpretation of Pushkin et al.[61] Despite of the aforementioned numerical issues associated with low-order methods, he employed a first-order Euler integrator with a relatively small time step. No particle–boundary interaction model was explicitly mentioned by Lappa.[31] In a successive study,[67] Lappa investigated the effect of g-jitter on the accumulation of particles in liquid bridges. In order to take into account the effect of the time-dependence of the flow field on the particle trajectories a far more complex version of the Maxey–Riley equation was employed. Using the same numerical approach as in his previous study, he found a wealth of different particle coherent structures depending on the amplitude and frequency of the g-jitter acceleration. In a private communication with one of the present authors (H. C. K.), Lappa clarified that his works[31,67] were carried out using a peculiar particle–boundary interaction model, not explicitly mentioned in the two articles. In his approach a variant of the PSI model with $\Delta = a$ was used for inelastic particle–boundary interactions all along the solid walls, whereas the particle–free surface interactions are treated as inelastic only in a narrow region near the hot and the cold rods. In a following paper, Lappa[68] investigated the accumulation of particles in liquid bridges when the flow arises as a standing hydrothermal wave. To explain the particle coherent structures found, the argument about axial vorticity and wave-interference dynamics was iterated. Unfortunately, again no mention was made of the treatment of the particle motion near the boundaries.

The debate between Shevtsova's and Kuhlmann's group about the physical mechanism responsible for the particle-accumulation phenomenon continued with Kuhlmann and Muldoon.[69] They commented on Melnikov et al.,[59] stating that the phase-locking mechanism cannot apply, because the necessary conditions for synchronization are not satisfied. In their rebuttal, Melnikov et al.[70] argued that the hydrothermal wave can be regarded as the weak force needed by the particulate dynamical system to synchronize. They do not explain, however, which weak coupling feedback is exerted by the particulate system on the fluid flow. It is clear, however, that their one-way-coupled simulations, intended as a proof of principle, exclude the feedback of the particles on the fluid flow.

Melnikov et al.[50] investigated the effect of the filling factor $\mathscr{V}$ on the formation of particle accumulation structures with $m = 2$ in a n-decane liquid bridge. In a follow-up study, Gotoda et al.[51] carried out additional experiments in n-decane liquid bridges, making use of particles of different radii a and density ratios ρ. They found that line-like accumulation structures such as SL1 and SL2 PAS can each be global attractors for the particle suspension. But for certain parameters they can also coexist, such that all particles are finally attracted to either of the two structures. An important result of their experimental study is the assessment of the importance of particle–particle interactions. It was observed that the coherent structures forming for individual monodisperse suspensions of particles of two different sizes might not form when the two kinds of particles are combined in a polydisperse suspension. Furthermore, they observed a periodic behavior of the particulate structure during which it vanishes and reappears periodically. In their most recent work on particle attractors in liquid bridges, Melnikov and Shevtsova[71] considered particles which are almost density-matched to the liquid. Their one-way-coupled numerical simulations included the collision model of Hofmann and Kuhlmann,[17] either on all boundaries or on the solid support rods only. Different from their previous studies, Melnikov and Shevtsova[71] described the particles to be in synchronous motion with the fluid flow, i.e. the particle dynamics is slaved to the flow, rather than claiming phase-locking of particle and flow by means of synchronization. They addressed the particle–boundary collision as well as the particle inertia as possible causes of the PAS obtained and confirmed that particles may accumulate faster due to the collisions than due to inertia.

5.3 Ueno's group

The group of Ueno has inherited the experience regarding PAS of Kawamura's research group and significantly extended the work. Kawamura et al.[48] reported the depletion of particles in the near-axis region inside the liquid bridge. This depletion mechanism was explained almost a decade later by Kuhlmann and Muldoon[21] by taking into account the streamline hopping experienced by the particles when they interact with the free surface, an effect numerically taken into account by the PSI model. The same kind of depletion patterns are documented in Kawamura et al.[72] and Ueno et al.,[32] who reported several accumulation patterns and classified the flow into eight different regimes according to the observed particle patterns. In a following study, Noguchi et al.[47] reported the depletion zones, the line-like particle coherent structures and also a quasi-axisymmetric toroidal core of particles, which is most likely hollow and is very similar to the toroidal shell observed under subcritical conditions. The toroidal core of particles can be transient or persistent depending on the flow and particle parameters. The study is also of technical

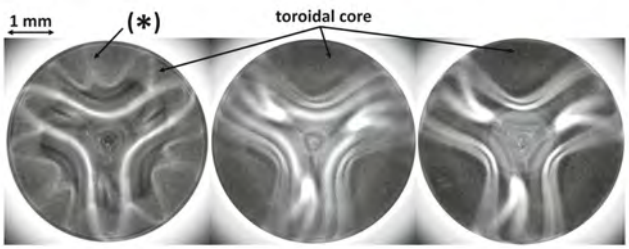

Fig. 5 Coaxial views on PAS through the transparent heated rod. Left: SL1 PAS wrapping around a toroidal core, middle: SL1 and period-doubled SL2 PAS, right: period-doubled SL2 PAS. The images, reproduced from Toyama et al.,[25] show 500 frames of a video record averaged in the rotating frame of reference. The hydrothermal wave and PAS co-rotate in counterclockwise direction.

significance, since three-dimensional particle-tracking velocimetry (3D-PTV) to characterize the particle accumulation has been introduced for the first time. Along the same line, the study of Nishimura et al.[73] is to be mentioned.

The important study of Tanaka et al.,[15] carried out in collaboration with Schwabe's group, has already been mentioned in section 5.1. In the same year, a review article of Kawamura and Ueno[74] on thermocapillary liquid bridges includes a section about accumulation of particles. The 3D-PTV technique elaborated by Noguchi et al.[47] was further exploited by Abe et al.,[75] who studied the effect of the filling factor $\mathscr{V}$ on the accumulation patterns. They reported a slight change of the attractor shape, while the fundamental line-like accumulation patterns remained a robust feature for $0.8 < \mathscr{V} < 1.2$. Along the same line of investigation are the publications of Ueno et al.[76] and Abe et al.[77] In the review papers of Kawamura et al.[78,79] the accumulation of particles in thermocapillary liquid bridges is presented as one of the primary scientific topics of the space experiment MEIS-1 of JASMA. Another parametric study about the accumulation of particles in liquid bridges was carried out by Niigaki and Ueno,[80] who also investigated the effect on PAS of a co-axial flow in the ambient gas phase. The two topics, PAS and the influence of an ambient gas flow on the thermocapillary convection, are the primary objectives of the planned Japanese–European space experiment JEREMI.

The particle accumulation in high-Prandtl-number liquid bridges (2-cSt silicone oil, $\mathrm{Pr} = 28$) was investigated by Gotoda et al.[81] They mounted a coaxial cylindrical shield around the liquid bridge, a method originally used by Preisser et al.,[82] to reduce external perturbations from the gas phase. Under supercritical conditions and when the thermocapillary Reynolds number is not to large, Gotoda et al.[81] found a toroidal core of particles in addition to the usual particulate coherent structures. Moreover, they measured the formation time of line-like structures to be $\approx d^2/\kappa$. This result, obtained for $\mathrm{Pr} = 28$, is larger than what was measured by Schwabe et al.[16] for lower-Prandtl-number liquid bridges. We stress, however, that the formation time of PAS cannot be directly correlated with the thermal diffusion time, since the thermal diffusion does not directly enter in the dynamical system of the particle motion (10). The publication of Gotoda et al.[51] on experiments with n-decane ($m = 2$) resulted from a collaboration between Ueno's and Shevtsova's group (see section 5.2). In a following study, Gotoda et al.[23] went back to 2-cSt-silicone-oil liquid bridges ($m = 3$), varying the thermocapillary Reynolds number in small steps and making use of particles with two different diameters (15 and 30 μm) and different densities. Upon an increase of Re, the characteristic depletion zone near the axis is observed in the particle suspension. Further increasing Re, the particle depletion pattern evolves into the core of particles and finally into SL1 PAS. If the Reynolds number is too high, the SL1 attractor disappears. Among the most interesting findings of Gotoda et al.[23] is a period-doubled coherent structure which was numerically predicted before by Mukin and Kuhlmann.[22] Another important result of Gotoda et al.[23] is the experimental proof of the correlation between PAS and the fluid flow. The authors found that the accumulation of the particle is synchronous to the flow. Moreover, the focusing of the particles to the line-like attractor is not correlated with the cold spot of the hydrothermal wave on the free surface, as was speculated by Schwabe et al.[16] Along the same line of Gotoda et al.,[23] Toyama et al.[25] investigated the existence range of SL1 and SL2 PAS depending on Ma, Γ and a. They confirmed that SL1 and SL2 PAS can coexist for certain parameter combination, or arise individually as global attractors (fig. 5). The formation times of the accumulation patterns were measured and, once again, the free surface temperature was monitored to characterize the phase relation between PAS and the hydrothermal wave.

5.4 Kuhlmann's group

The research carried out in Kuhlmann's group makes frequent use of dynamical system theory to place PAS in a more general and solid theoretical framework. Their first investigation[83] studied the effect of added mass, pressure gradient, Stokes drag and buoyancy for particles in a Taylor–Green vortex with $\rho = 2$. Their main result was the characterization of limit cycles for the particulate dynamical system and, upon an increase of the Stokes number, they find a period-doubling sequence which follows the Feigenbaum scenario. A following paper of Domesi[84] introduced a fully elastic particle–boundary interaction model, which was used to compute the accumulation of particles in subcritical thermocapillary liquid bridges. A different modeling approach was taken by Hofmann and Kuhlmann,[17] who treated the particle–boundary interaction as an inelastic collision which dissipates the particle kinetic energy in normal-to-boundary direction. They introduced the PSI model used in most of the numerical studies (not only of Kuhlmann's group) and which can

be considered an approximation to the particle–free-surface interaction which has turned out to be a key factor for PAS. Making use of the stationarity of the fluid flow in a reference frame rotating with the hydrothermal wave, Hofmann and Kuhlmann[17] transformed the SMR equation into the rotating frame of reference. The particle trajectories were then integrated in the rotating frame, utilizing that the particles do not affect the flow in one-way coupling. This approach provides an enormous saving of computational resources and is used in all the numerical investigations of Kuhlmann's group. Another important advance of Hofmann and Kuhlmann[17] was to link the particle accumulation to the flow topology and, in particular, to the Kolmogorov–Arnol'd–Moser (KAM) tori, which very closely resemble the particle attractors. The groundwork theory proposed in Hofmann and Kuhlmann[17] explained the accumulation phenomenon as a transfer of particles from the chaotic to the regular regions (KAM tori) of the flow, made possible by the particle–boundary interaction. This interpretation of PAS does not rely on the particle inertia and well explains the accumulation of density-matched particles experimentally observed by Schwabe et al.[16] An in-depth investigation of the role of the KAM tori and the focussing mechanism of particles inside of the KAM tori, as well as the role for PAS of the particle size was also carried out by Hofmann and Kuhlmann.[17]

Inspired by the model flow of Pushkin et al.,[61] the results of which have been discussed in Sec. 5.2, Kuhlmann and Muldoon[64] proposed a flow field in closed-form which was fitted to the numerically simulated flow in a thermocapillary liquid bridge for $\mathrm{Pr} = 4$ and $\mathrm{Re} = 1800$. Employing their new model flow, Kuhlmann and Muldoon[85] explained in detail the particle accumulation mechanism due to particle–boundary interactions, discussing the necessary conditions to observe line-like coherent structures. In a following study, Muldoon and Kuhlmann[21] used their model flow to further investigate the accumulation of particles in the liquid bridge. They carried out an extensive analysis in terms of particle radius, explained particle depletion zones as a phenomenon produced by the particle–boundary interaction and predicted line-like, tubular and strange PAS. Multiple PAS as well as a simply periodic particle attractor with fundamental wave number $m = 1$ was also predicted by Muldoon and Kuhlmann[21], similar to the one later found by Gotoda et al.[51] Furthermore, a quantity K, based on box counting, was introduced to measure the instantaneous degree of particle segregation in order to mathematically define the formation time of PAS. In a subsequent study Muldoon and Kuhlmann[41] pointed out the important role of numerical error accumulation in computing particle trajectories. The corresponding implications for low-order integration schemes have been discussed above.

Mukin and Kuhlmann[22] accurately characterized the numerical flow topology, in the rotating reference frame for $\mathrm{Pr} = 4$ and three supercritical Reynolds numbers. The accumulation of density-matched particles was analyzed for $\mathrm{Re} = 1800$ as function of the interaction length Δ of the PSI model which is the only parameter of this model. The accumulation of particles was explained in correlation with the reconstructed KAM tori of the flow, within which the line-like attractors are typically located. Moreover, the period-doubling of the particle attractor was predicted for moderately large particles. The reason for the period doubling was explained within the framework of the advection equation ($\dot{\mathbf{y}} = \mathbf{u}$) supplemented by the PSI model. Additional simulations of purely advected particles which interact with all the boundaries according to the PSI model are reported in Muldoon and Kuhlmann,[86] who varied the interaction length Δ to investigate all the possible accumulation patterns which are predicted for the particulate dynamical system in dependence on the particle radius. Several qualitatively different coherent structures were reported upon an increase of Δ.

A joint paper[87] by scientists from all groups working on PAS gives a very brief overview on the different results obtained at that time. Kuhlmann et al.[88] pointed out that the streamline crowding near the driving boundary of the liquid bridge (free surface) is a flow feature which tends to promote PAS. Comparing the formation times of coherent structures induced by inertia with those by particle–free-surface collisions, it was concluded that the experimental results of Schwabe et al.[16] can only be explained if the particle–boundary interaction is taken into account. Pure inertial attraction was found to have a formation time which is two orders of magnitude larger than what is measured experimentally. The same conclusion was drawn for the accumulation of particles reported in the other experiments: the experimental time scale is compatible with collision-induced particle accumulation and not with inertial coherent structures. Kuhlmann et al.[88] also transformed the experimental videos from the laboratory to the rotating frame of reference and time-averaged over many individual video frames to ease the comparison of experimental results with numerical predictions. This post-processing technique has now become a standard procedure for the global visualization of PAS in liquid-bridge experiments. Another analysis of the time scale of PAS is due to Kuhlmann and Lemée,[89] who considered the temporal evolution of the depletion zone, correlating the turnover time of individual particles in the axisymmetric part of the model flow of Muldoon and Kuhlmann[21] with the evolution of the depletion volume. The resulting time scale estimate was found to well agree with the experimental time scales measured by Schwabe et al.[16] The most recent numerical study of particle accumulation in liquid bridges with $\mathrm{Pr} = 4$ was carried out by Muldoon and Kuhlmann,[24] who systematically varied the particle radius and the particle-to-fluid density ratio. For $\Delta = 0$ they retrieved the inertial time scale such that their accumulation measure $K(t)$ becomes universal when the time is rescaled $t \to t' = t|\rho - 1|St/\rho$, yielding an inertial formation time $\sim \rho/(|\rho - 1|St)$. This is consistent with the findings of Kuhlmann et al.[88] and confirms that the experimentally reported accumula-

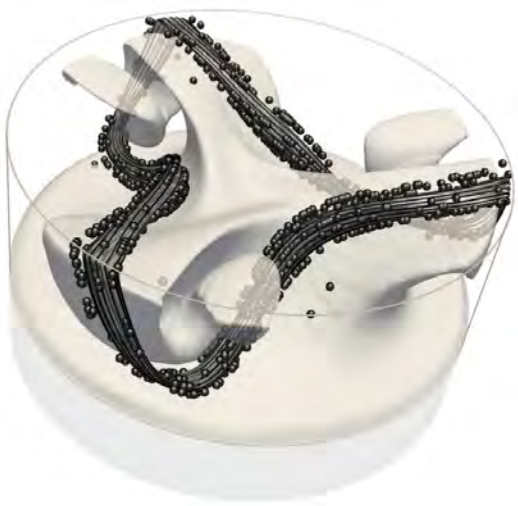

Fig. 6 A finite-size Lagrangian coherent structure (PAS) made by 1000 particles (dark spheres) forms in a thin KAM torus (not shown) slightly outside of the main KAM torus (dark-gray) for $\Delta = 0.00552$, $\Gamma = 0.68$, $\mathrm{Re} = 1600$ and $\mathrm{Pr} = 28$. The temperature iso-surface $\theta = 1/2$ (light-gray) of the hydrothermal wave is strongly affected by the flow. The structure is shown at $t = 3d^2/\kappa$ after particle initialization at random positions. The figure is taken from Romanò and Kuhlmann.[26)]

tion structures cannot be explained as inertial coherent structures, in particular, not in the limit $\rho \to 1$. When the PSI model is activated, the coherent particle structures form much more rapidly, consistent with the experimental data. Moreover, Muldoon and Kuhlmann[24)] investigated the effect of the artificial boundary conditions used by Lappa[67)] and found that the accumulation patterns reported in Lappa's studies might be a mere result of the fictitious boundary repulsion on strips of the free surface introduced by the author to prevent the particles from leaving the domain.

Romanò and Kuhlmann[29)] carried out fully-resolved simulations of particles near moving walls and shear surfaces. They considered two-dimensional flows and numerically resolved all the relevant scales of the flow: the macroscopic fluid flow scale ($\sim d$), the particle scale ($\sim a$), and the lubrication length scale δ of the gap between the particle's surface and the indeformable boundary. Their fully-resolved calculations revealed that the particle centroid indeed moves a wide distance nearly parallel to the tangentially moving boundary with a minimum distance $\Delta = a + \delta$. This result confirmed that the PSI model can be intended as a zeroth-order approximation to the actual particle–boundary dynamics, giving physical motivation to the inelastic collision approach. Considering $\rho = 2$, they found that a particle in a shear-driven square cavity with $\mathrm{Re} = 1000$ is displaced away from the moving boundary even more than what is predicted by the model of Hofmann and Kuhlmann[17)] who assumed $\Delta = a$. This confirmed the hypothesis that the lubrication gap δ between the particle surface and the boundaries may not be negligible. In a following study Romanò and Kuhlmann[18)] carried out fully-resolved simulations of a particle in a shear-driven square cavity for $\mathrm{Re} = 1000$ and $\mathrm{Pr} \to 0$. Both, the particle radius and the particle-to-fluid density ratio were targeted. Considering particles slightly heavier than the fluid, they computed the two-dimensional particle attractors and proposed a fit of the fully-resolved minimum lubrication gap $\delta(a, \rho)$ as function of the particle radius a and the particle-to-fluid density ratio ρ. These fits were used to determine the scalar parameter Δ of the PSI model. Using the interaction parameter Δ obtained in this way, the trajectories from the one-way-coupled simulations were in very good agreement with the trajectories from the fully-resolved simulations. A further confirmation of the correlations proposed by Romanò and Kuhlmann[18)] was reported in Romanò et al.,[20)] who compared one-way-coupled simulations of a particle in a subcritical liquid bridge with corresponding experiments, well predicting the most important characteristic parameters of the particle attractor, i.e. its minimum and maximum radial coordinate.

The most recent publications on PAS in thermocapillary liquid bridges are due to Romanò and Kuhlmann.[26,27)] In Ref.[26)] the Lagrangian topology of a high-Prandtl-number fluid flow ($\mathrm{Pr} = 28.5$) was obtained in the frame of reference rotating with the hydrothermal wave. These results allowed, for the first time, to compare numerical simulations with the abundant experimental results of Ueno's group for 2 cSt silicone oil. The strong correlation between flow topology and particle attractors was, once again, confirmed and the numerical predictions of PAS of Romanò and Kuhlmann[26)] (see fig. 6) agreed very well with the coherent structures measured by Toyama et al.[25)] With help of the flow topology, Romanò and Kuhlmann[26)] could explain why SL1 and SL2 PAS coexist for $\mathrm{Re} = 1850$: There is a narrow window of Reynolds numbers within which two KAM tori coexist, ${}^1T_3^3$ and ${}^1T_3^6$, which very well resemble the SL1 and SL2 particle attractors, respectively. For $\mathrm{Re} = 1600$ and $\mathrm{Re} = 1750$ only SL1 PAS is observed, since the fluid flow topology admits only the ${}^1T_3^3$ KAM torus. On the other hand, for $\mathrm{Re} = 1950$ only SL2 PAS is experimentally reported, because only the ${}^1T_3^6$ KAM torus is present.

As another important result, Romanò and Kuhlmann[26)] could prove that the accumulation of particles found in the experiments of Ueno's group are essentially due to particle–free-surface interaction and that inertial effects are of very minor significance. Even excluding inertial forces from the particle motion model, the simulations of Romanò and Kuhlmann[26)] well capture the experimental observations. This led the authors to coin the new term of *finite-size coherent structures* (FSCS). This terminology is used to emphasize that the accumulation of particles in small thermocapillary liquid bridges is caused by an essentially non-inertial mechanism. As should have become clear, this mechanism is based on the particle size. This is qualitatively different from the well-known inertial coherent structures.[40)] Moreover, FSCS

indicates that the particle attractors are strongly coherent, which is not very well expressed by the established name PAS. Another aspect which speaks in favor of FSCS is its more general importance also in other flow systems with non-thermocapillary surface forces. Theoretical aspects of FSCS are discussed in Romanò et al.,[27] where a generalization of FSCS is proposed to a whole subclass of all boundary-driven flows.

6. Phenomenology of FSCS

Having summarized the literature on particle accumulation in liquid bridges, we now give a brief description of the essential ingredients to FSCS in three-dimensional, steady, incompressible flows. Since the flow properties and the mechanisms of particle accumulation leading to FSCS are not restricted to the flow in thermocapillary liquid bridges, the more general character of FSCS becomes clear.

As proven by the studies of Kuhlmann's group, the correlation between flow topology (where does a fluid element go?) and coherent particle structures (where does a particle go?) is crucial for understanding FSCS. A key feature of the flow topology in any three-dimensional, steady, incompressible flow is that the trajectories of fluid elements (streamlines in steady flow) are either chaotic or regular.[90] The flow does not need to be steady in the laboratory frame, is suffices that the flow is steady in some frame of reference (e.g., rotating or translating). Chaotic streamlines depend sensitively on the initial condition, while regular streamlines are periodic or quasi-periodic. For two-dimensional steady flow all streamlines are regular (periodic in a closed system). As the flow becomes three-dimensional, e.g. by a hydrodynamic instability, part of the streamlines become chaotic. Typically, there exists a range of Reynolds numbers in which chaotic and regular streamlines coexist, and where the regular, quasi-periodic streamlines arise in the form of KAM tori. Both types of streamlines are important for FSCS: in the region of chaotic streamlines (chaotic sea) fluid elements are usually well mixed, and, based on the ergodicity assumption, any fluid element from the chaotic region will visit the whole subvolume occupied by chaotic streamlines. On the contrary, fluid elements do not get well mixed in the regular regions of the flow, because any fluid element is restricted to move on a single KAM torus. Therefore, the fluid contained in the regular regions is sealed from the fluid in the chaotic region(s).

The property of the fluid being sealed in the KAM tori is inherited by a suspended particle, if it moves like a tracer, i.e. if it is convected, satisfying $\dot{\mathbf{y}} = \mathbf{u}$. While this is not exactly the case, it is a very good assumption if $\mathrm{St} \ll 1$, $\rho = \mathcal{O}(1)$, if buoyancy forces are small (e.g. under microgravity conditions) and the particle moves far away from the boundaries. Also each particle of an ensemble of particles nearly moves like the fluid, if the particle-to-fluid volume ratio is $\phi \ll 1$ and particle–particle interactions can be neglected (if the local density of particles remains small). In this case, the dynamics of the suspension can be modeled as a superposition of multiple single-particle dynamics. Under these conditions, particles initially located in the chaotic sea tend to explore, in the course of time, the whole chaotic sea. Particles initially located in a KAM torus of the flow tend to remain in the KAM torus. If all particles would perfectly inherit the motion of fluid elements, particle accumulation would be impossible, because of the incompressibility of the flow $\nabla \cdot \mathbf{u} = 0$. In fact, a three-dimensional, steady, incompressible flow is equivalent to a piecewise Hamiltonian with 1.5 degrees of freedom[91] and, hence, cannot admit any accumulation. Therefore, small deviations of the particle trajectories from those of fluid elements are necessary for the existence of FSCS.

Deviations of particle trajectories from trajectories of fluid elements can arise in the bulk for finite-size particles. However, these deviations vanish as the particle size tends to zero $a \to 0$, but remains finite with $a \neq 0$. In this limit, which differs from setting $a = 0$, particles are advected in the bulk, but not near the boundaries, where the particle size must be taken into account inside a boundary layer of size $\mathcal{O}(a)$. The situation is conceptually similar to Prandtl's boundary layer, where viscosity can be neglected everywhere, except for a thin boundary layer on the wall. Therefore, the trajectories of small particles deviate from trajectories of fluid elements near indeformable boundaries. In thermocapillary liquid bridges this effect is important near the free surface, because the streamlines are crowed there. The deviation of the particle trajectories from those of fluid elements near a boundary causes particles originally moving in the chaotic sea to be transferred to a regular region. The details of this process have been explained by Hofmann and Kuhlmann.[17] Such a transfer, however, is possible only if a KAM torus exists which enters the boundary layer of thickness $\mathcal{O}(a)$ which can receive the particles. Once a particle has entered a KAM torus it can be trapped there forever. Exceptions and complications are discussed in Mukin and Kuhlmann.[22]

In the above approximation FSCS can be understood as the attraction of individual particles to a periodic or quasi-periodic trajectory. The single particle process can also be understood in the framework of dynamical systems: If the particle–boundary interaction in the layer of thickness $\mathcal{O}(a)$ is absent, the phase space of the particle motion is identical to the physical space occupied by the liquid, because specifying the initial location of the particle defines its trajectory for all times. In that case the dynamical system is Hamiltonian, attractors do not exist and the divergence of the flux in phase space is zero: $\nabla \cdot \dot{\mathbf{y}} = \nabla \cdot \mathbf{u} = 0$. The particle–boundary interaction, however, introduces a dissipation, because the particle experiences a normal-to-wall drag force in the boundary layer, which is a sink of kinetic energy of the particle. This makes the dynamical system dissipative such that attractors of the particle motion come into existence. Note, the conditions for the existence of a FSCS are independent of whether the flow system is a thermocapillary liquid bridge or not, the above conditions can

be satisfied by a whole class of flows.

We would like to point out that the concept of FSCS as a single particle process must be extended, if the system becomes more complex. A modification is required if, e.g., the density of particles is too large globally or locally (as in the final stage of the FSCS) such that particle–particle interactions can no longer be neglected. For instance, the destruction of FSCS experimentally observed by Gotoda et al.[51] could be caused by particle–particle interactions. Another aspect not included in the above simplified scenario is the dissipation due to the particle–boundary interaction may be strong enough to create attracting orbits even in weakly chaotic regions of the flow (characterized by small Lyapunov exponents), as was observed by Kuhlmann and Muldoon[92] and Romanò and Kuhlmann.[26]

7. FSCS in other flow systems

In a number of microsystems, particle accumulations have been reported which can be classified as FSCS. For instance, the trapping of cells, bacteria and particles in micro-channels and biofilms has been reported by Yazdi and Ardekani[93] and Karimi and Ardekani.[94] In their experiments, particles were found to accumulate in the streaming flow near the surface of a rapidly oscillating gas bubble. Other examples of FSCS in bio-microfluidics were reported by Wang et al.,[95,96] who also used streaming flows. They suggested FSCS as an effective size-sensitive sorting mechanism for particles moving near boundaries.

Finite-size coherent structures have been found also in lid-driven cavities by Romanò[101] and Kuhlmann et al.,[102] who achieved a very good agreement between numerical predictions of the particle motion and corresponding particle-tracking experiments. Another experimental evidence for FSCS in lid-driven cavities was provided by Wu et al.,[103], again pointing out the strong correlation between FSCS and fluid flow topology. Along the same line, Romanò et al.[27] reported an excellent comparison between experimental particle tracking and one-way-coupled numerical simulations carried out using either the SMR equation (10) or perfect advection for modeling the particle motion in the bulk of the cavity. In both the cases, the particle-motion model was supplemented with the PSI model when the particle moves close to a boundary. The most recent study about FSCS in the lid-driven cavity is due to Romanò et al.[104], who numerically demonstrated the creation of coherent particle structures in a two-sided lid-driven cavity. For the first time, a continuous particle–boundary interaction model derived from lubrication theory has been implemented. Switching the particle–boundary interaction on and off, the time scales for the formation of inertial coherent structures could be compared with that of finite-size coherent structures.

Recently, FSCS have been reported for other thermocapillary-driven systems. Orlishausen et al.[105] investigated the quasi-two-dimensional FSCS in a shear-driven micro-reactor, in a suspension of nano-particles. Last but not least, Takakusagi et al.[106] reported the accumulation of particles in pending thermocapillary droplets, heated from the ceiling and cooled from the gas phase.

8. Future Perspectives

Two decades of research resulted in the understanding of the particle accumulation phenomenon in liquid bridges. A solid theoretical background has been developed, together with the notion on finite-size coherent structures. However, some important questions are still open.

As an obvious improvement, a more realistic particle–boundary interaction model is desirable. The current discontinuous collision model should be replaced by a continuous and smooth interaction which captures, at least, the enhanced normal-to-boundary viscous drag in the particle boundary layer. It can be expected that such an improved modeling will allow better estimates of the time scales on which FSCS evolve than is currently possible with the PSI model. The study of Romanò et al.[104] is a first step forward in this direction.

Another major issue which needs further investigation is the role of particle–particle interaction. The massive attraction of particles to their common single-particle attractor locally increases the density of particles on and near the periodic or quasi-periodic single-particle orbit, violating the fundamental hypothesis of independent particles. Including interaction forces among the particles would also allow to investigate polydisperse suspensions in liquid bridges and, eventually, lead to a deeper understanding of the experimentally observed destruction of FSCS.[51] The binary particle–particle interaction may be modeled by taking into account at least the viscous forces exerted along the line connecting the particle centroids when they move closer than some threshold value. A good starting point for the modeling is represented by the exact Stokes-flow solution provided by Stimson and Jeffery[107] for two spherical particles of arbitrary radius moving against each other.

Finally, an important open question is related to the effect of particle perturbations of the flow topology. This issue becomes more urgent the higher the local particle concentration gets and the larger the particle size is compared to the flow domain. To take into account the particle-induced changes of the flow the current one-way coupling needs to be replaced, at least, by a two-way-coupling approach. It can be expected that the KAM structure of the flow topology is destroyed, but the essential transport properties may approximately survive in some parameter ranges. In two way coupling the use of a single snapshot of the flow field of a hydrothermal wave, however, can no longer be used and one has to resort to a more computationally intensive approach, similar to the one adopted by Shevtsova's group.

Acknowledgements

Support by ESA through contract number 4000121111/17/NL/PG/pt is gratefully acknowledged.

References

1) A. G. Kidanemariam and M. Uhlmann: J. Fluid Mech., **750** (2014) R2.
2) F. Amato, M. Pandolfi, T. Moreno, M. Furger, J. Pey, A. Alastuey, N. Bukowiecki, A. S. H. Prevot, U. Baltensperger and X. Querol: Atmos. Environ., **45** (2011) 6777–6787.
3) A. Mali and A. Ataie: Ceram. Int., **30** (2004) 1979–1983.
4) J. Rieger, T. Frechen, G. Cox, W. Heckmann, C. Schmidt and J. Thieme: Faraday Discuss., **136** (2007) 265–277.
5) M. B. Dolovich and R. Dhand: The Lancet, **377** (2011) 1032–1045.
6) J. Zhang, S. Yan, D. Yuan, G. Alici, N.-T. Nguyen, M. E. Warkiani and W. Li: Lab Chip, **16** (2016) 10–34.
7) A. Babiano, J. H. E. Cartwright, O. Piro and A. Provenzale: Phys. Rev. Let., **84** (2000) 5764–5767.
8) T. Sapsis and G. Haller: J. Atm. Sci., **66** (2009) 2481–2492.
9) F. Romanò: J. Fluid Mech., **857** (2018) R3.
10) H. Brenner: Chem. Eng. Sci., **16** (1961) 242–251.
11) D. Schwabe, P. Hintz and S. Frank: Microgravity Sci. Technol., **9** (1996) 163–168.
12) M.Wanschura, V. S. Shevtsova, H. C. Kuhlmann and H. J. Rath: Phys. Fluids, **7** (1995) 912–925.
13) J. Leypoldt, H. C. Kuhlmann and H. J. Rath: J. Fluid Mech., **414** (2000) 285–314.
14) J. Leypoldt, H. C. Kuhlmann and H. J. Rath: Adv. Space Res., **29** (2002) 645–650.
15) S. Tanaka, H. Kawamura, I. Ueno and D. Schwabe: Phys. Fluids, **18** (2006) 067103.
16) D. Schwabe, A. I. Mizev, M. Udhayasankar and S. Tanaka: Phys. Fluids, **19** (2007) 072102.
17) E. Hofmann and H. C. Kuhlmann: Phys. Fluids, **23** (2011) 0721106.
18) F. Romanò and H. C. Kuhlmann: Theor. Comput. Fluid Dyn., **31** (2017) 427–445.
19) F. Romanò and H. C. Kuhlmann: Int. J. Num. Meth. Fluids, **83** (2017) 485–512.
20) F. Romanò, H. C. Kuhlmann, M. Ishimura and I. Ueno: Phys. Fluids, **29** (2017) 093303.
21) F. H. Muldoon and H. C. Kuhlmann: Physica D, **253** (2013) 40–65.
22) R. V. Mukin and H. C. Kuhlmann: Phys. Rev. E, **88** (2013) 053016.
23) M. Gotoda, A. Toyama, M. Ishimura, T. Sano, M. Suzuki, T. Kaneko and I. Ueno: **private communication**.
24) F. H. Muldoon and H. C. Kuhlmann: Phys. Fluids, **28** (2016) 073305.
25) A. Toyama, M. Gotoda, T. Kaneko and I. Ueno: Microgravity Sci. Technol., **29** (2017) 263–274.
26) F. Romanò and H. C. Kuhlmann: Phys. Rev. Fluids, **3** (2018) 094302.
27) F. Romanò, H. Wu and H. C. Kuhlmann: Int. J. Multiphase Flow, **111** (2019) 42–52.
28) F. Romanò and H. C. Kuhlmann: Proc. Appl. Math. Mech., **15** (2015) 519–520.
29) F. Romanò and H. C. Kuhlmann: Int. J. Heat Fluid Flow, **62** (2016) 75–82.
30) D. Melnikov, D. Pushkin and V. Shevtsova: Eur. Phys. J. Special Topics, **192** (2011) 29–39.
31) M. Lappa: Phys. Fluids, **25** (2013) 012101.
32) I. Ueno, S. Tanaka and H. Kawamura: Phys. Fluids, **15** (2003) 408–416.
33) T. Yano, K. Nishino, I. Ueno, S. Matsumoto and Y. Kamotani: Phys. Fluids, **29** (2017) 044105.
34) H. C. Kuhlmann and C. Nienhüser: Fluid Dyn. Res., **31** (2002) 103–127.
35) F. Romanò and H. C. Kuhlmann: Tech. Mech., **39** (2019) 71–83.
36) J. F. Padday: Phil. Trans. R. Soc. Lond. A, **269** (1971) 265–293.
37) Y. Gaponenko and V. Shevtsova: Microgravity Sci. Technol., **24** (2012) 297–306.
38) M. R. Maxey and J. J. Riley: Phys. Fluids, **26** (1983) 883–889.
39) T. Peacock and J. Dabiri: Chaos, **20** (2010) 017501.
40) G. Haller: Annu. Rev. Fluid Mech., **47** (2015) 137–162.
41) F. H. Muldoon and H. C. Kuhlmann: Comput. Fluids, **88** (2013) 43–50.
42) J. Bohm, A. Lüdge and W. Schröder: In Handbook of Crystal Growth, ed. D. T. J. Hurle, vol. 2a (Basic Techniques), North Holland, 1994, 213–257.
43) A. Cröll, W. Müller-Sebert, K. W. Benz and R. Nitsche: Microgravity Sci. Technol., **3** (1991) 204–215.
44) D. Schwabe, A. Scharmann, F. Preisser and F. Oeder: J. Crystal Growth, **43** (1978) 305–312.
45) D. Schwabe, S. Tanaka, A. Mizev and H. Kawamura: Microgravity Sci. Technol., **18** (2006) 117–127.
46) H. Kawamura, K. Nishino, M. Yamamoto, S. Yoda, T. Nakamura, T. S. Morita, K. Kawasaki and H. Tamaoki: J. Jpn. Soc. Microgravity Appl., **14** (1997) 34–41.
47) K. Noguchi, I. Ueno, S. Tanaka, H. Kawamura and K. Nishino: 11th Iinternational Symposium on Flow Visualization, USA, August 2004.
48) H. Kawamura, I. Ueno, S. Tanaka and D. Nagano: 2nd International Symposium on Turbulence and Shear-Flow Phenomena, Sweden, June 2001, 375–380.
49) I. Ueno, Y. Ono, D. Nagano, S. Tanaka and H. Kawamura: 4th JSME-KSME Therm. Eng. Conf., vol. 3, Jpn. Soc. Mech. Eng., Kobe, Japan, 2000, 265–270.
50) D. E. Melnikov, T. Watanabe, T. Matsugase, I. Ueno, V. Shevtsova: Microgravity Sci. Technol., **26** (2014) 365–374.
51) M. Gotoda, D. E. Melnikov, I. Ueno and V. Shevtsova: Chaos, **26** (2016) 073106.
52) Y. Gaponenko, A. Miadlun and V. Shevtsova: Eur. Phys. J. Special Topics, **192** (2011) 63–70.
53) Y. Gaponenko, A. Mialdun and V. Shevtsova: Int. J. Multiphase Flow, **39** (2012) 205–215.
54) V. Yasnou, Y. Gaponenko, A. Mialdun and V. Shevtsova: Int. J. Heat Mass Transfer, **123** (2018) 747–759.
55) D. Schwabe: Second European Symposium on the Utilization of the ISS, ESA SP-433, The Netherlands, 233-240, 1999.
56) D. Schwabe and S. Frank: Adv. Space Res., **23** (1999) 1191–1196.
57) D. Schwabe und S. Frank: Adv. Space Res., **24** (1999) 1391–1396.
58) D. Schwabe and A. I. Mizev: Eur. Phys. J. Special Topics, **192** (2011) 13–27.
59) D. E. Melnikov, D. O. Pushkin and V. M. Shevtsova: Phys. Fluids, **25** (2013) 092108.
60) D. Schwabe: Microgravity Sci. Technol., **26** (2014) 1–10.
61) D. O. Pushkin, D. E. Melnikov and V. M. Shevtsova: Phys. Rev. Lett., **106** (2011) 234501.

62) J. C. Lasheras and K.-K. Tio: Appl. Mech. Rev., **47** (1994) S61.
63) H. C. Kuhlmann and F. H. Muldoon: Phys. Rev. Lett., **108** (2012) 249401.
64) H. C. Kuhlmann and F. H. Muldoon: Phys. Rev. E, **85** (2012) 046310.
65) D. O. Pushkin, D. E. Melnikov and V. M. Shevtsova: Phys. Rev. Lett., **108** (2012) 249402.
66) D. E. Melnikov, T. Takakusagi, D. O. Pushkin and V. M. Shevtsova: J. Jpn. Soc. Microgravity Appl., **29** (2012) 77–83.
67) M. Lappa: J. Fluid Mech., **726** (2013) 160–195.
68) M. Lappa: Phys. Fluids, **26** (2014) 093301.
69) H. C. Kuhlmann and F. H. Muldoon: Phys. Fluids, **26** (2014) 099101.
70) D. E. Melnikov, D. O. Pushkin and V. Shevtsova: Phys. Fluids, **26** (2014) 099102.
71) D. E. Melnikov and V. Shevtsova: Eur. Phys. J. Special Topics, **226** (2017) 1239–1251.
72) H. Kawamura, I. Ueno and T. Ishikawa: Adv. Space Res., **29** (2002) 611–618.
73) M. Nishimura, I. Ueno, K. Nishino and H. Kawamura: Exp. Fluids, **38** (2005) 285–290.
74) H. Kawamura and I. Ueno: Surface Tension-Driven Flows and Applications, ed. R. Savino, 1–24, Research Signpost, India, 2006.
75) Y. Abe, I. Ueno and H. Kawamura: Microgravity Sci. Technol., **19** (2007) 84–86.
76) I. Ueno, Y. Abe, K. Noguchi and H. Kawamura: Adv. Space Res., **41** (2008) 2145–2149.
77) Y. Abe, I. Ueno and H. Kawamura: Ann. N.Y. Acad. Sci., **1161** (2009) 240–245.
78) H. Kawamura, K. Nishino, S. Matsumoto and I. Ueno: 14th International Heat Transfer Conference, USA, August 2010, 343–362.
79) H. Kawamura, K. Nishino, S. Matsumoto and I. Ueno: J. Heat Transfer, **134** (2012) 031005.
80) Y. Niigaki and I. Ueno: Trans. JSASS Aerospace Tech. Japan, **10** (2012) Ph_33–Ph_37.
81) M. Gotoda, T. Sano, T. Kaneko and I. Ueno: Eur. Phys. J. Special Topics, **224** (2015) 299–307.
82) F. Preisser, D. Schwabe and A. Scharmann: J. Fluid Mech., **126** (1983) 545–567.
83) S. Domesi and H. C. Kuhlmann: Proc. Appl. Math. Mech., **5** (2005) 593–594.
84) S. Domesi: Microgravity Sci. Technol., **18** (2006) 137–140.
85) H. C. Kuhlmann and F. H. Muldoon: J. Jpn. Soc. Microgravity Appl., **29** (2012) 64–76.
86) F. H. Muldoon and H. C. Kuhlmann: Int. J. Multiphase Flow, **59** (2014) 145–159.
87) H. C. Kuhlmann, M. Lappa, D. Melnikov, R. Mukin, F. H. Muldoon, D. Pushkin, V. Shevtsova and I. Ueno: Fluid Dyn. Mat. Proc., **10** (2014) 1–36.
88) H. C. Kuhlmann, R. V. Mukin, T. Sano and I. Ueno: Fluid Dyn. Res., **46** (2014) 041421.
89) H. C. Kuhlmann and T. Lemée: Eur. Phys. J. Special Topics, **224** (2015) 309–318.
90) J. M. Ottino: Mixing, chaotic advection, and turbulence. Annu. Rev. Fluid Mech. **22** (1990), 207–254.
91) K. Bajer: Chaos Soliton. Fract., **4** (1994) 895–911.
92) H. C. Kuhlmann and F. H. Muldoon: Eur. Phys. J. Special Topics, **219** (2013) 59–69.
93) S. Yazdi and A. M. Ardekani: Biomicrofluidics, **6** (2012) 044114.
94) A. Karimi, S. Yazdi and A. M. Ardekani: Biomicrofluidics, **7** (2013) 021501.
95) C. Wang, S. V. Jalikop and S. Hilgenfeldt: Appl. Phys. Lett., **99** (2011) 034101.
96) C. Wang, S. V. Jalikop and S. Hilgenfeldt: Biomicrofluidics, **6** (2012) 012801.
97) M. Lappa: Chaos, **23** (2013) 013105.
98) M. Lappa: Phys. Fluids, **26** (2014) 013305.
99) M. Lappa: Geophys. Astrophys. Fluid Dyn., **110** (2016) 348–386.
100) M. Lappa: Int. J. Multiphase Flow, **93** (2017) 71–83.
101) F. Romanò: Ph.D. Thesis, TU Wien (2016).
102) H. C. Kuhlmann, F. Romanò, H. Wu and S. Albensoeder: 20th Australasian Fluid Mechanics Conference, December 2016, Australia, paper no. 449, 102.
103) H. Wu, F. Romanò and H. C. Kuhlmann: Proc. Appl. Math. Mech., **17** (2017) 669–670.
104) F. Romanò, P. Kunchi Kannan and H. C. Kuhlmann: Phys. Rev. Fluids, **4** (2019) 024302.
105) M. Orlishausen, L. Butzhammer, D. Schlotbohm, D. Zapf and W. Köhler: Soft Matter, **13** (2017) 7053–7060.
106) T. Takakusagi and I. Ueno: Langmuir, **33** (2017) 13197–13206.
107) M. Stimson and G. B. Jeffery: Proc. R. Soc. Lond. A, **111** (1926) 110–116.